



# Non-isothermal study of gasification process of coal char and biomass char in CO<sub>2</sub> condition

Tao Xu<sup>1</sup>, Guang-wei Wang<sup>1,\*</sup>, Jian-liang Zhang<sup>1</sup>, Teng-fei Song<sup>1</sup>, Run-sheng Xu<sup>2</sup>

<sup>1</sup> School of Metallurgical and Ecological Engineering, University of Science and Technology Beijing, Beijing 100083, China

<sup>2</sup> School of Materials and Metallurgy, Wuhan University of Science and Technology, Wuhan 430081, Hubei, China

## ARTICLE INFO

### Key words:

Coal char  
Biomass char  
Gasification  
Kinetic model

## ABSTRACT

Non-isothermal method was used to study gasification characteristics of three coal chars and one biomass char. Four chars were made from anthracite coal (A), bituminous coal (B), lignite coal (L), and wood refuse (W), respectively. The gasification process was studied by random pore model (RPM), unreacted core model (URCM) and volumetric model (VM). With an increase in metamorphic grade, the gasification reactivity of coal char decreased, and the gasification reactivity of biomass char was close to that of low metamorphic coal char. With an increase in heating rate, the gasification of all samples moved towards high temperature zone, and the whole gasification time decreased. It was concluded from kinetics analysis that the above-mentioned three models could be used to describe the gasification process of coal char, and the RPM fitted the best among the three models. In the RPM, the activation energies of gasification were 193.9, 225.3 and 202.8 kJ/mol for anthracite coal char, bituminous coal char and lignite coal char, respectively. The gasification process of biomass char could be described by the URCM and VM, while the URCM performed better. The activation energy of gasification of wood refuse char calculated by the URCM was 282.0 kJ/mol.

## Symbol List

$C$ —Concentration of reaction gas;  
 $E$ —Apparent activation energy;  
 $k$ —Apparent reaction rate constant;  
 $k_0$ —Pre-exponential factor;  
 $L_0$ —Hole length;  
 $m_0$ —Initial mass of sample;  
 $m_\infty$ —Final mass of sample;  
 $m_t$ —Mass of sample at time  $t$ ;  
 $n$ —Reaction order;  
 $R$ —Universal gas constant;  
 $R^2$ —Correlation coefficient;

$S_0$ —Specific surface area;  
 $t$ —Reaction time;  
 $T$ —Temperature;  
 $T_0$ —Reaction starting temperature;  
 $\alpha$ —Char gasification conversion rate;  
 $f(\alpha)$ —Function of mechanism of reaction kinetics;  
 $\beta$ —Heating rate;  
 $\delta$ —Relative error;  
 $\epsilon_0$ —Solid porosity;  
 $\psi$ —Parameter of particle structure.

## 1. Introduction

With the improvement of environmental protection and the development of clean coal technology, coal gasification technology has received great attention through the world<sup>[1–3]</sup>. At the same time, biomass is regarded as a carbon-neutral fuel when it is burned. Thus, biomass is considered as an effective alternative fuel to fossil fuel for reducing the greenhouse gas emission<sup>[4]</sup>. The gasification kinetics of coal is an important factor that affects the clean con-

version and the utilization of coal. And the gasification reaction of CO<sub>2</sub> with char is the most important in the whole process of gasification reaction of coal. Scholars have done a lot of research on the kinetic process of gasification reaction<sup>[5–12]</sup>. The gasification behavior of biomass has been widely investigated. Wang et al.<sup>[13]</sup> studied the CO<sub>2</sub> gasification properties and kinetics of biomass chars including four kinds of herbaceous residues and two kinds of wooden residues, and found that gasification reactivity of char was mostly determined by its carbonaceous

\* Corresponding author. Ph.D.

E-mail address: wgw676@163.com (G.W. Wang).

structure. Okumura et al.<sup>[14]</sup> studied the influence of pyrolysis conditions on woody biomass char reactivity. The relationship between the biomass char characteristics and the gasification rates was found.

Thermogravimetric analysis is widely used in the gasification reaction, which can determine the kinetic parameters of chemical reactions, as well as the transition temperatures of chemical reaction control and air diffusion control. The usual methods used in the thermogravimetric analysis are isothermal method and non-isothermal method. The former describes the overall reactivity of char at specific temperature and the latter reflects the variation regularity of the gasification reaction in the whole process of coal char with increasing temperature. Compared with isothermal method, non-isothermal method has the characteristics of a small amount of experiments, a short operating period, and more information, etc.<sup>[15]</sup>. In the practical production process, the reaction temperature is affected by multiple factors so that it hardly remains stable.

Thus, the CO<sub>2</sub> gasification reaction characteristics were analyzed by non-isothermal thermogravimetry and the effects of coal quality and heating rate on gasification reaction of coal char and biomass char were investigated. Finally, the random pore model (RPM)<sup>[16,17]</sup>, unreacted core model (URCM)<sup>[18]</sup> and volumetric model (VM)<sup>[19,20]</sup> were used to calculate the kinetic parameters of the gasification reaction.

## 2. Experimental

### 2.1. Raw material

Anthracite coal, bituminous coal, lignite coal and wood refuse (labeled as A, B, L, and W) were obtained from an enterprise. The results of proximate analysis and elemental analysis of samples are shown in Table 1. Before the experiment, the samples were dried in an oven at 105 °C for 4 h, and then broken. The coal samples were ground to 0.074 mm for carbonization. The waste wood was sawed into 10 mm × 10 mm × 10 mm block for carbonization. The samples were carbonized at 1000 °C for 60 min in N<sub>2</sub> gas

**Table 1**  
Proximate and ultimate analysis of different samples (wt. %)

Sample	Proximate analysis				Ultimate analysis			
	FC <sub>d</sub>	A <sub>d</sub>	V <sub>d</sub>	C <sub>d</sub>	H <sub>d</sub>	O <sub>d</sub>	N <sub>d</sub>	S <sub>d</sub>
A	70.43	14.69	14.88	75.23	2.50	1.61	0.93	0.85
B	50.42	16.85	32.73	61.21	5.91	11.80	3.03	0.86
C	35.37	8.87	55.76	60.76	2.76	13.87	0.64	0.19
D	16.39	0.45	83.16	48.04	5.06	39.77	0.37	0.06

Note: 1) FC, A, and V refer to fixed carbon, ash and volatile matter, respectively, and subscript d means in dry basis; 2) FC and O are calculated by difference.

atmosphere using a tube furnace, and then cooled to room temperature. Biomass char was ground under 0.074 mm. Four kinds of chars made by anthracite coal, bituminous coal, lignite coal and wood refuse were labeled as AC, BC, LC and WC, respectively.

### 2.2. Experimental process

The gasification reaction of coal char and biomass chars was measured by using a thermogravimetric analyzer (HCT-3 Henven Scientific Instrument Factory, Beijing). (5.0 ± 0.1) mg of sample was put into an alumina crucible (ϕ3.0 mm × 1.5 mm). The flow rate of 99.9% carbon dioxide was 60 mL/min. The heating rate was set to be 2.5, 5 and 10 °C/min by non-isothermal method to study the characteristics of the chars. The gasification conversion rates of coal char and biomass char were calculated by the computer automatically recorded curves of mass loss, as shown in Eq. (1).

$$\alpha = \frac{(m_0 - m_t)}{(m_0 - m_\infty)} \quad (1)$$

## 3. Dynamic Model

In the process of non-catalytic gas-solid reaction, the oxidative decomposition reaction kinetics equation can be expressed as:

$$\frac{d\alpha}{dt} = k(P_g, T)f(\alpha) \quad (2)$$

where,  $k$  includes the effects of reaction temperature and partial pressure in the gas phase  $P_g$ .

It is assumed that gaseous pressure of the samples in the process remains constant and the apparent reaction rate constant of the samples is mainly influenced by the reaction temperature, and the form can be expressed by the Arrhenius formula:

$$k = k_0 e^{-E/(RT)} \quad (3)$$

In this paper, three kinds of gas-solid reaction kinetic models, RPM, URCM and VM, were used to study the chemical reaction kinetics of coal char and biomass char in CO<sub>2</sub> atmosphere. The expressions of reaction rate can be expressed as:

$$\frac{d\alpha}{dt} = k_{RPM}(1-\alpha)\sqrt{1-\phi}\ln(1-\alpha) \quad (4)$$

$$\frac{d\alpha}{dt} = k_{URCM}(1-\alpha)^{2/3} \quad (5)$$

$$\frac{d\alpha}{dt} = k_{VM}(1-\alpha) \quad (6)$$

where,

$$\phi = \frac{4\pi L_0(1-\epsilon_0)}{S_0^2} \quad (7)$$

$k_{RPM}$ ,  $k_{URCM}$  and  $k_{VM}$  are the reaction rate constants of three kinds of gasification reaction models, respectively.

Under the non-isothermal or temperature-programmed conditions, there was a relationship among

the reaction temperature, the heating rate and the reaction time:

$$T = T_0 + \beta t \tag{8}$$

By combining Eqs. (4) and (8),

$$\alpha = 1 - \exp\left\{-\frac{k_{RPM} C^n S_0}{1 - \epsilon_0} \cdot \frac{(T - T_0)}{\beta}\right\} \cdot \left[1 + \frac{4\pi L_0 k_{RPM} C^n}{S_0} \cdot \frac{(T - T_0)}{\beta}\right] \tag{9}$$

By combining Eqs. (3) and (9),

$$\alpha = 1 - \exp\left\{-\left[A_0 \cdot \frac{(T - T_0)}{\beta} \cdot \exp\left(\frac{-E}{RT}\right)\right]\right\} \cdot \left[1 + A_1 \cdot \frac{(T - T_0)}{\beta} \cdot \exp\left(\frac{-E}{RT}\right)\right] \tag{10}$$

where,  $A_0 = \frac{k_0 C^n S_0}{1 - \epsilon_0}$ ,  $A_1 = \frac{\pi L_0 k_0 C^n}{S_0}$ .

Similarly, Eqs. (5) and (6) can be transformed into:

$$\alpha = 1 - \left[1 - \frac{k_0 (T - T_0)}{3\beta} \cdot \exp\left(\frac{-E}{RT}\right)\right]^3 \tag{11}$$

$$\alpha = 1 - \exp\left[-k_0 \frac{(T - T_0)}{\beta} \cdot \exp\left(\frac{-E}{RT}\right)\right] \tag{12}$$

According to the relation of  $\alpha$  and  $T$  from Eqs. (10), (11) and (12), the kinetic parameters  $k_0$  and  $E$  can be calculated by nonlinear fitting method.

Based on the description of coal char and biomass char gasification kinetics under different assumptions by the three models, the errors between the calculated value and the actual value are inevitable. In order to accurately determine the description of the coal char and biomass char gasification kinetics with different

kinetic models, Eq. (13) can be used to calculate the relative error of the results of different models.

$$\delta = 100 \times \frac{\left[\sum_{i=1}^N (\alpha_{exp,i} - \alpha_{calc,i})^2 / N\right]^{1/2}}{\max(\alpha)_{exp}} \tag{13}$$

where,  $\alpha_{exp,i}$  and  $\alpha_{calc,i}$  are the experimental data and calculated value, respectively;  $\max(\alpha)_{exp}$  is the maximum conversion rate of experiment; and  $N$  is the number of experimental points.

## 4. Results and Discussion

### 4.1. Gasification characteristics of coal char and biomass char

The conversion rate curves and mass loss rate curves of four kinds of chars in the CO<sub>2</sub> atmosphere are shown in Fig. 1. Obviously, the mass loss curves of these four kinds of chars after gasification reaction process were similar. The gasification reaction process consisted of three stages, which were the heating-up stage, the gasification stage, and the complete gasification stage. It was similar to the process of determining coal combustion characteristic parameter by using conversion rate curve and mass loss rate curve to get initial gasification temperature ( $T_i$ ), total gasification temperature ( $T_f$ ), maximum gasification rate ( $R_m$ ), temperature of maximum gasification rate ( $T_m$ ), and gasification time  $t_g$ , etc. [21], which can determine the performance of char gasification. Gasification reaction characteristic parameters of four kinds of chars are shown in Table 2.

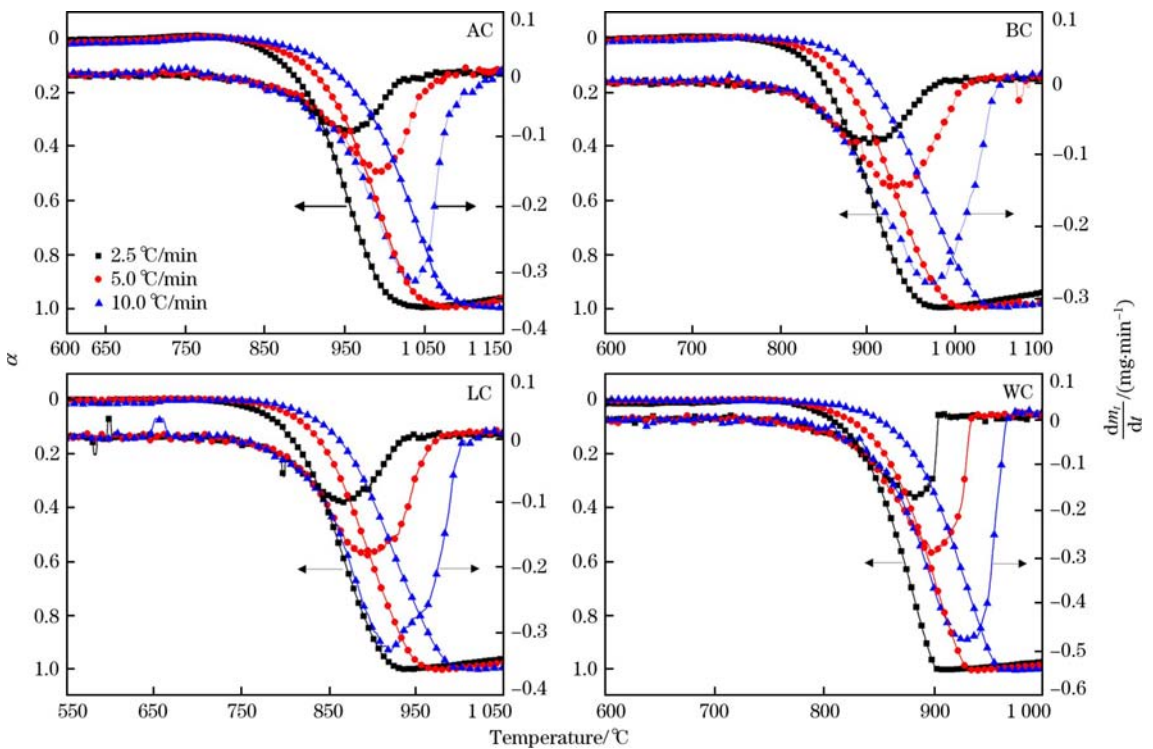


Fig. 1. Conversion and reaction rate curves of coal chars and biomass char at different heating rates.

**Table 2**  
Characteristic gasification parameters of coal char and biomass char at different heating rates

Char	$\beta/$ ( $^{\circ}\text{C} \cdot \text{min}^{-1}$ )	$T_i/$ $^{\circ}\text{C}$	$T_m/$ $^{\circ}\text{C}$	$T_f/$ $^{\circ}\text{C}$	$R_m/$ ( $\text{mg} \cdot \text{min}^{-1}$ )	$t_g/$ min
AC	2.5	829.7	954.1	1018.9	0.086	75.7
	5.0	846.2	990.6	1054.1	0.148	41.6
	10	862.7	1034.5	1092.5	0.318	23.0
LC	2.5	751.9	862.0	917.9	0.099	66.4
	5.0	779.0	892.9	950.0	0.182	34.2
	10	798.0	918.9	982.9	0.330	18.5
BC	2.5	796.0	903.9	962.0	0.083	66.4
	5.0	815.9	935.9	992.9	0.145	35.4
	10	837.0	971.0	1025.9	0.282	19.0
WC	2.5	779.1	884.0	899.2	0.170	48.0
	5.0	795.9	899.2	927.2	0.290	26.2
	10	816.7	928.0	954.4	0.477	13.8

With the increase of coal rank,  $T_i$  and  $T_f$  increased gradually when heating at  $10^{\circ}\text{C}/\text{min}$  for the three kinds of coal samples. Thus, it could be concluded that the gasification reactivity of three kinds of coal chars can be ranked as:  $\text{LC} > \text{BC} > \text{AC}$ . The gasification reactivity of coal char reduced with the increase of coal rank reported in literatures<sup>[22,23]</sup>. At  $10^{\circ}\text{C}/\text{min}$ ,  $T_i$  and  $T_f$  were  $816.7$  and  $954.4^{\circ}\text{C}$  for biomass char, respectively. The gasification reactivity of biomass char was analogous to that of LC, while better than that of AC.

Comparing the effects of different heating rates on the mass loss curve of four kinds of samples, with the increase of heating rate, the conversion rate curve and the mass loss rate curve moved towards high temperature region and the peak value of mass loss rate increased gradually. Moreover, the thermal hysteresis effect of the sample became more remarkable, which caused the char gasification process to move into higher temperature region. Taking AC as an example, as the heating rate increased from  $2.5$  to  $10^{\circ}\text{C}/\text{min}$ ,  $T_i$  ranged from  $829.7$  to  $862.7^{\circ}\text{C}$ ,  $R_m$  increased from  $0.086$  to  $0.318 \text{ mg}/\text{min}$ , and the gasification reaction time decreased from  $75.7$  to  $23.0$  min.

#### 4.2. Kinetic analysis

According to Chapter 3, gasification kinetic parameters ( $E$ ,  $k_0$ ,  $\psi$  and  $R^2$ ) were calculated using

RPM, URCM and VM, as listed in Table 3. Using three models for AC, BC and LC, it showed a good correlation between calculated and experimental values ( $R^2 > 0.999$ ).  $R^2$  of the RPM was  $0.9997$ , which was higher than that of URCM and VM. Among the three models, the URCM was best fitted for the WC reaction whose fitting error  $R^2$  was  $0.9991$ . Conversely, VM and RPM could not describe the relationship between experimental data and calculated value of WC well. The value of  $\psi$  has a significant impact on the calculation results. With the decrease of  $\psi$ , the sample particle porosity became bigger and sample gasification reaction process was closer to the physical assumption by the RPM. With the increase of  $\psi$ , the sample particle porosity became smaller, resulting in a greater resistance of gas through the particle surface into the particle interior. Thus, the URCM was suitable to simulate the sample gasification reaction process. The space structure of biomass char was well developed because of the special structure of plant cell walls. The typical structure of biomass char was honeycomb thin-walled tube where tube section generally showed a regular hexagon<sup>[24]</sup>. Meanwhile, thin-walled tube surface was smooth, with less micro gap. After crushed, the thin-walled structure was broken, leading to the decrease of the porosity of biomass char. The structure was closer to the physical assumption of the URCM.

According to Table 3, the order of three gasification models to calculate the activation energy was consistent for different samples (except RPM calculation of activation energy of biomass char). The order of activation energy could be ranked as  $\text{WC} > \text{BC} > \text{LC} > \text{AC}$ . It indicated that under the experimental conditions, temperature had an important effect on the biomass char WC, while had the least influence on anthracite char. Under the same condition,  $k_0$  (including  $k_{\text{RPM}}$ ,  $k_{\text{URCM}}$ , and  $k_{\text{VM}}$ ) based on three different models had the same order, i. e.  $\text{WC} > \text{BC} > \text{LC} > \text{AC}$ . The results suggested that all these three dynamic models could reflect the coal and biomass gasification reaction kinetic characteristics, and could be applied to calculate the kinetic parameters. It should be pointed out that the higher the gasification reactivity, the higher was the activity energy, as shown in Table 3. The main reason for this pheno-

**Table 3**  
Kinetic parameters of chars at three heating rates for RPM, URCM and VM

Char	RPM				URCM			VM		
	$E/$ ( $\text{kJ} \cdot \text{mol}^{-1}$ )	$k_{\text{RPM}}/$ $\text{min}^{-1}$	$\psi$	$R^2$	$E/$ ( $\text{kJ} \cdot \text{mol}^{-1}$ )	$k_{\text{URCM}}/$ $\text{min}^{-1}$	$R^2$	$E/$ ( $\text{kJ} \cdot \text{mol}^{-1}$ )	$k_{\text{VM}}/$ $\text{min}^{-1}$	$R^2$
AC	193.9	$2.76 \times 10^4$	1.83	0.9999	185.4	$4.93 \times 10^3$	0.9994	219.3	$4.70 \times 10^5$	0.9990
BC	225.3	$1.56 \times 10^6$	0.56	0.9998	214.2	$1.62 \times 10^5$	0.9995	242.1	$9.53 \times 10^6$	0.9996
LC	202.8	$3.70 \times 10^5$	0.80	0.9997	197.1	$6.74 \times 10^4$	0.9996	223.1	$3.57 \times 10^6$	0.9994
WC	205.2	$2.07 \times 10^3$	$3.20 \times 10^5$	0.9918	285.0	$6.08 \times 10^8$	0.9991	315.3	$4.99 \times 10^{10}$	0.9969

menon was that the gasification reactivity was affected both by the activity energies and by the pre-exponential factors. Comparing the activation energy and the pre-exponential factors of different samples, the pre-exponential factors increased with the activity energies, which was the so-called kinetic compensation effect, as reported previously<sup>[25,26]</sup>. In order to screen out the most fitted kinetics calculation model, the relative error between the calculated value and the experimental value was used to evaluate these three models.

Fig. 2 shows the relationship between the calculated and experimental values of different samples at three heating rates. For AC, BC and LC chars, calculated values were essentially coincident with the experimental curve using three kinds of models. However, the differences of calculated and experimental values for biomass char WC varied greatly. Eq. (12) was used to calculate the relative error between the experimental and calculated values. The calculated results based on Eq. (12) for all samples are listed in Table 4. The error value based on the RPM

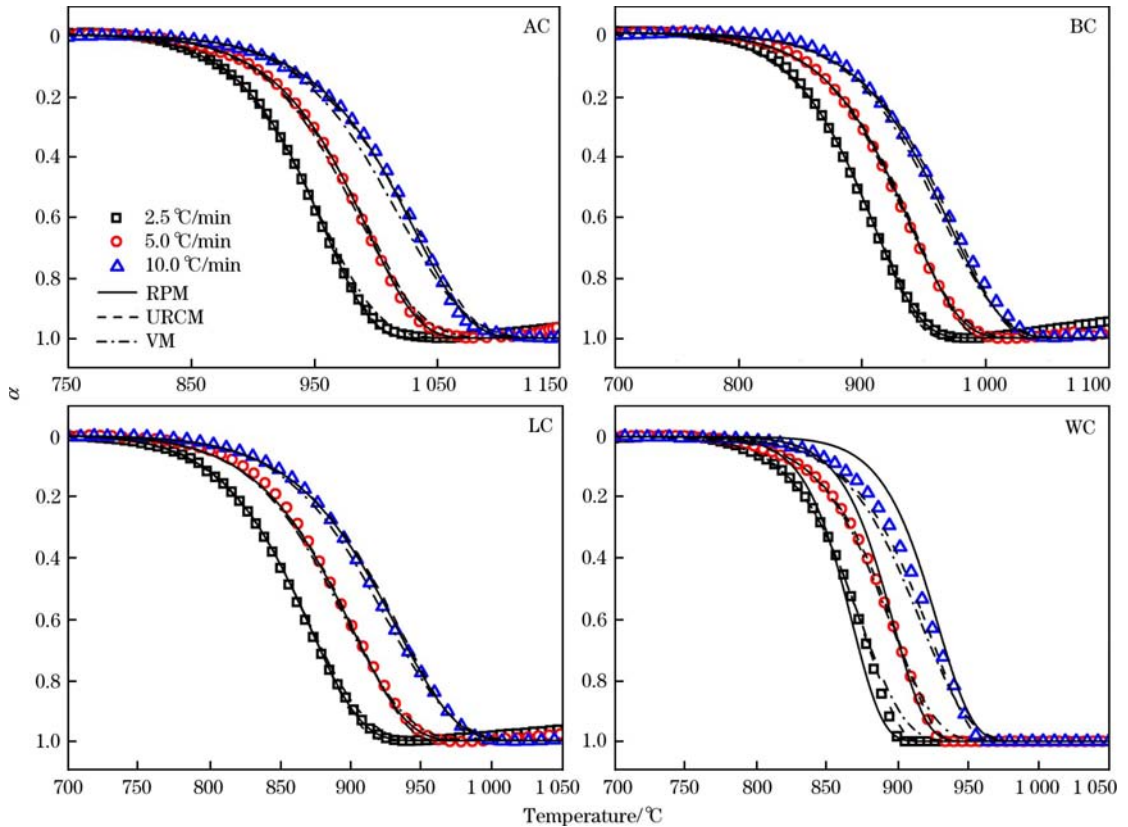


Fig. 2. Experimental conversion curves and calculation curves with gasification model at different heating rates.

Table 4  
Relative error between experimental and calculated conversion (%)

Char	RPM	URCM	VM
AC	0.61	1.35	1.82
BC	0.73	1.01	1.24
LC	0.89	1.28	1.17
WC	3.79	1.14	2.12

for AC, BC and LC chars was small, less than 1%, while for WC char, it was large, up to 3.79%. The minimum relative error calculated by the URCM was 1.14%. Therefore, the RPM was the most suitable for characterization of three kinds of coal chars in CO<sub>2</sub> gasification process and gasification activation energy for the AC, BC and LC char was 193.9,

225.3 and 202.8 kJ/mol, respectively; URCM was best fitted for biomass char in CO<sub>2</sub> gasification process, whose gasification activation energy was 285.0 kJ/mol.

### 5. Conclusions

(1) Char gasification reactivity was affected by the metamorphic degree of coal. The gasification reactivities for three kinds of coal chars decreased with increasing the metamorphic degree. The gasification reactivity of biomass char was close to that of the low metamorphic coal chars. The gasification reaction time was affected by heating rate because the reaction time was shortened owing to the increase of heating rate.

(2) The kinetics results suggested that RPM,

URCM and VM could be used to describe the gasification reaction process, while the simulation results of RPM for coal chars was the optimal. VM and URCM could be used to describe biomass char gasification process, while URCM was the optimal.

(3) The kinetic parameter calculation results showed that the four kinds of chars could be totally affected by the metamorphic degree. The apparent activation energy decreased with the increase of the metamorphic degree. The CO<sub>2</sub> gasification activation energies of AC, BC, LC and WC chars were calculated based on the optimal model, which were 193.9, 225.3, 202.8 and 285.0 kJ/mol, respectively.

## Acknowledgment

This work was supported by the China Postdoctoral Science Foundation (2016M600043) and the Fundamental Research Funds for the Central Universities (FRF-TP-15-063A1).

## References

- [1] J. Ding, Q. C. Liu, L. J. Jiang, G. Q. Liu, S. Ren, J. Yang, L. Yao, F. Meng, *J. Iron Steel Res. Int.* 23 (2016) 917-923.
- [2] J. Feroso, M. V. Gil, C. Pevida, J. J. Pis, F. Rubiera, *Chem. Eng. J.* 161 (2012) 276-284.
- [3] G. W. Wang, J. L. Zhang, J. G. Shao, H. Sun, H. B. Zuo, *J. Iron Steel Res. Int.* 21 (2014) 897-904.
- [4] J. G. M. S. Machado, E. Osorio, A. C. F. Vilela, A. Babich, D. Senk, H. W. Gudenau, *Steel Res. Int.* 81 (2010) 9-16.
- [5] D. P. Ye, J. B. Agnew, D. K. Zhang, *Fuel* 77 (1998) 1209-1219.
- [6] R. C. Everson, H. W. Neomagus, H. Kasaini, D. Njaphac, *Fuel* 85 (2006) 1076-1083.
- [7] J. L. Zhang, G. W. Wang, J. G. Shao, H. B. Zuo, *Bioresources* 9 (2014) 3497-3507.
- [8] G. W. Wang, J. L. Zhang, X. M. Hou, J. G. Shao, W. W. Geng, *Bioresour. Technol.* 177 (2015) 66-73.
- [9] S. Q. Xu, Z. J. Zhou, F. Yang, G. S. Yu, Z. H. Yu, *Proc. CSEE* 29 (2009) No. 2, 41-46 (in Chinese).
- [10] G. W. Wang, J. L. Zhang, J. G. Shao, Z. J. Liu, G. H. Zhang, T. Xu, J. Guo, H. Y. Wang, R. S. Xu, H. Lin, *Energy Convers. Manage.* 124 (2016) 414-426.
- [11] G. W. Wang, J. L. Zhang, J. G. Shao, S. Ren, *Thermochim. Acta* 591 (2014) 68-74.
- [12] F. Hua, S. Hu, J. Xiang, L. S. Sun, J. M. Shi, P. Fu, G. Chen, S. Su, *CIESC J.* 62 (2011) 199-205 (in Chinese).
- [13] G. W. Wang, J. L. Zhang, J. G. Shao, Z. J. Liu, H. Y. Wang, X. Y. Li, P. C. Zhang, W. W. Geng, G. H. Zhang, *Energy* 114 (2016) 143-154.
- [14] Y. Okumura, T. Hanaoka, K. Sakanishi, *Proc. Combust. Inst.* 32 (2009) 2013-2020.
- [15] Z. J. Zhou, X. L. Fan, W. Zhang, F. C. Wang, Z. H. Yu, *J. China Coal Soc.* 31 (2006) No. 2, 219-222 (in Chinese).
- [16] S. K. Bhatia, D. D. Perlmutter, *AIChE J.* 26 (1980) 379-385.
- [17] S. K. Bhatia, D. D. Perlmutter, *AIChE J.* 27 (1981) 247-254.
- [18] J. Ochoa, M. C. Cassanello, P. R. Bonelli, A. L. Cukierman, *Fuel Process. Technol.* 74 (2001) No. 12, 161-176.
- [19] S. Kasaoka, Y. Sakata, S. Kayano, C. Tong, *Int. Chem. Eng.* 25 (1984) 160-175.
- [20] J. Y. Shang, E. W. Eduardo, *Fuel* 63 (1984) 1640-1609.
- [21] Y. Xu, C. Zhang, J. Xia, Y. H. Duan, J. J. Yin, G. Chen, *Asia-Pacific J. Chem. Eng.* 3 (2010) 435-440.
- [22] Q. H. Pang, J. L. Zhang, R. Mao, Z. Jiang, T. Liu, *J. Iron Steel Res. Int.* 21 (2014) 312-320.
- [23] C. L. Qi, J. L. Zhang, X. H. Lin, Q. Y. Liu, X. L. Wang, *J. Iron Steel Res. Int.* 18 (2011) No. 8, 1-8.
- [24] Z. W. Hu, J. J. Zhang, H. B. Zuo, J. Li, Z. J. Liu, T. J. Yang, *J. Univ. Sci. Technol. Beijing* 34 (2012) 998-1005 (in Chinese).
- [25] G. W. Wang, J. L. Zhang, J. G. Shao, Y. K. Jiang, B. Gao, D. Zhao, D. H. Liu, H. Y. Wang, Z. J. Liu, K. X. Jiao, *Bioresources* 11 (2016) 4821-4838.
- [26] A. P. Dhupe, A. N. Gokarn, L. K. Doraiswamy, *Fuel* 70 (1991) 839-844.